

Electronic Supplementary Information (ESI) for Nanoscale

**Hierarchical assembly of hyaluronan coated cationic albumin nanoparticles for pancreatic cancer chemoimmunotherapy**

Ying Hu<sup>a,1</sup>, Xue Chen<sup>a,1</sup>, Yingying Xu<sup>a</sup>, Xianru Han<sup>a</sup>, Mou Wang<sup>a</sup>, Tao Gong<sup>a</sup>, Zhi-Rong Zhang<sup>a</sup>, W. John Kao<sup>b</sup>, Yao Fu<sup>a\*</sup>

<sup>a</sup> Key Laboratory of Drug Targeting and Drug Delivery System, Ministry of Education,  
West China School of Pharmacy, Sichuan University, Chengdu, 610041, China

<sup>b</sup> Department of Industrial and Manufacturing Systems Engineering, Biomedical Engineering, and Chemical  
Biology Centre, The University of Hong Kong, Pokfulam, HKSAR

<sup>1</sup> Co-first authors

\*Correspondence:

Yao Fu (Y. Fu)

Email: yfu4@scu.edu.cn (Y. Fu)

Tel: +86-28-65503798

Fax: +86-28-85501615

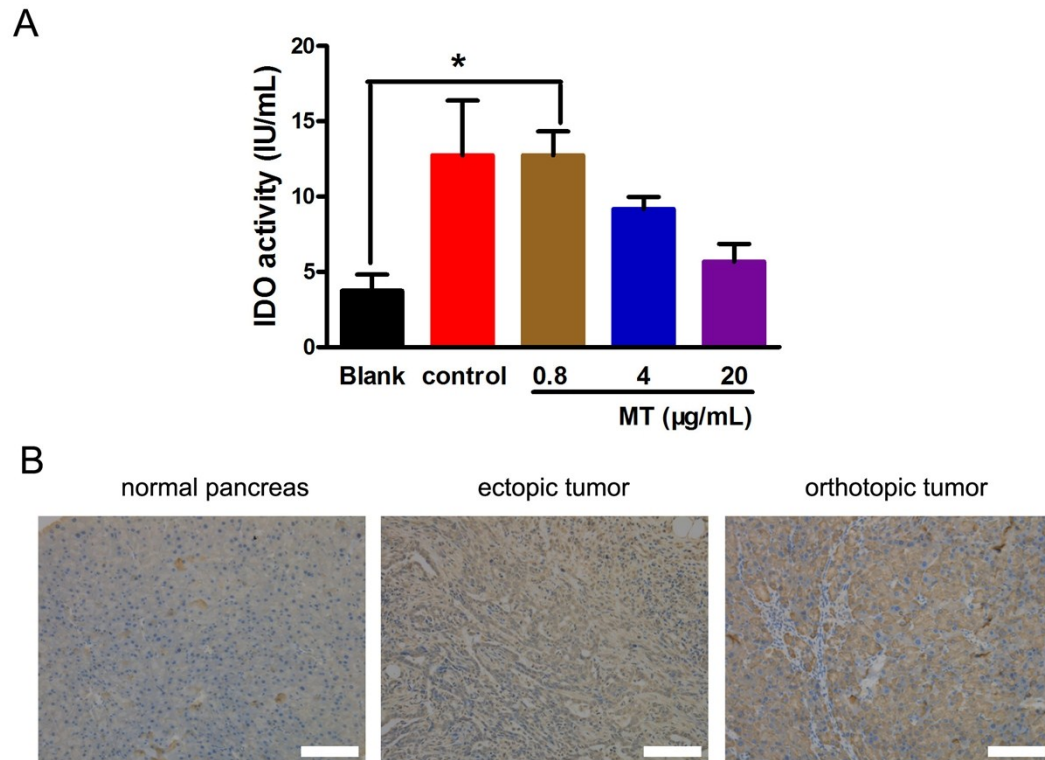


**Figure S1.** (A) Expression levels of Indoleamine-2,3-dioxygenase in Panc02 following treatments of MT with varying concentrations. (B) Immunohistochemical staining for IDO, Scale bars = 100 µm. Data represent mean  $\pm$  SD ( $n = 3$ ), \* $P < 0.05$ .

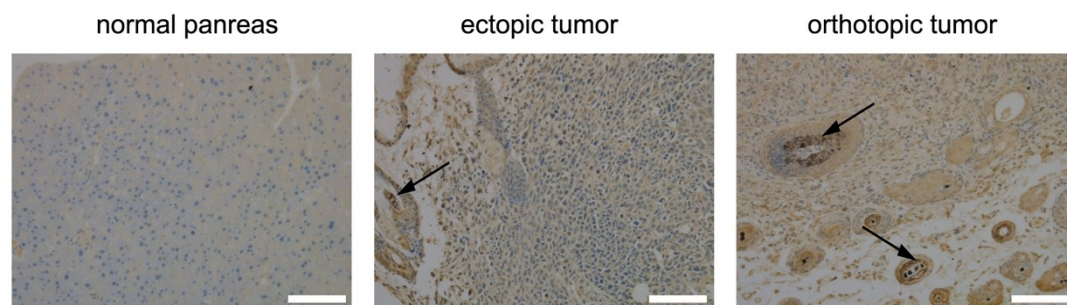


**Figure S2.** Immunohistochemical staining for CD44, Scale bars = 100 µm.

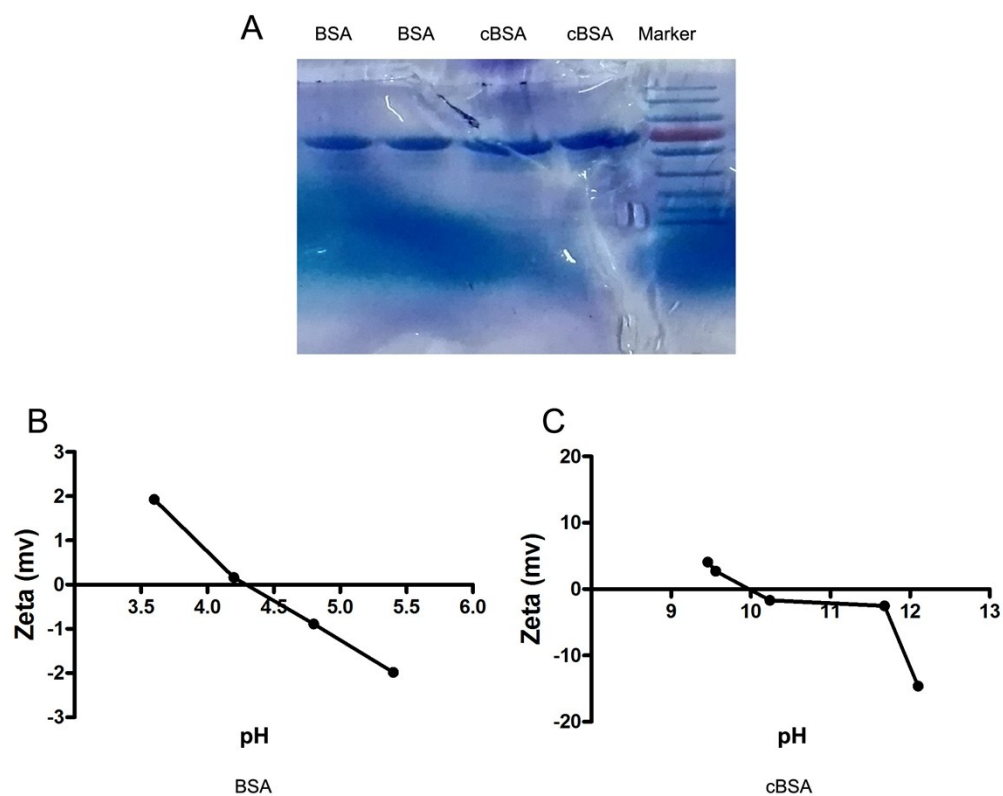


**Figure S3.** Characterization of BSA and cBSA by SDS-PAGE. (A) Separation of SDS-polypeptide chains of BSA and cBSA. (B) and (C) separately show the surface  $\zeta$  potential of BSA and cBSA in different pH condition.

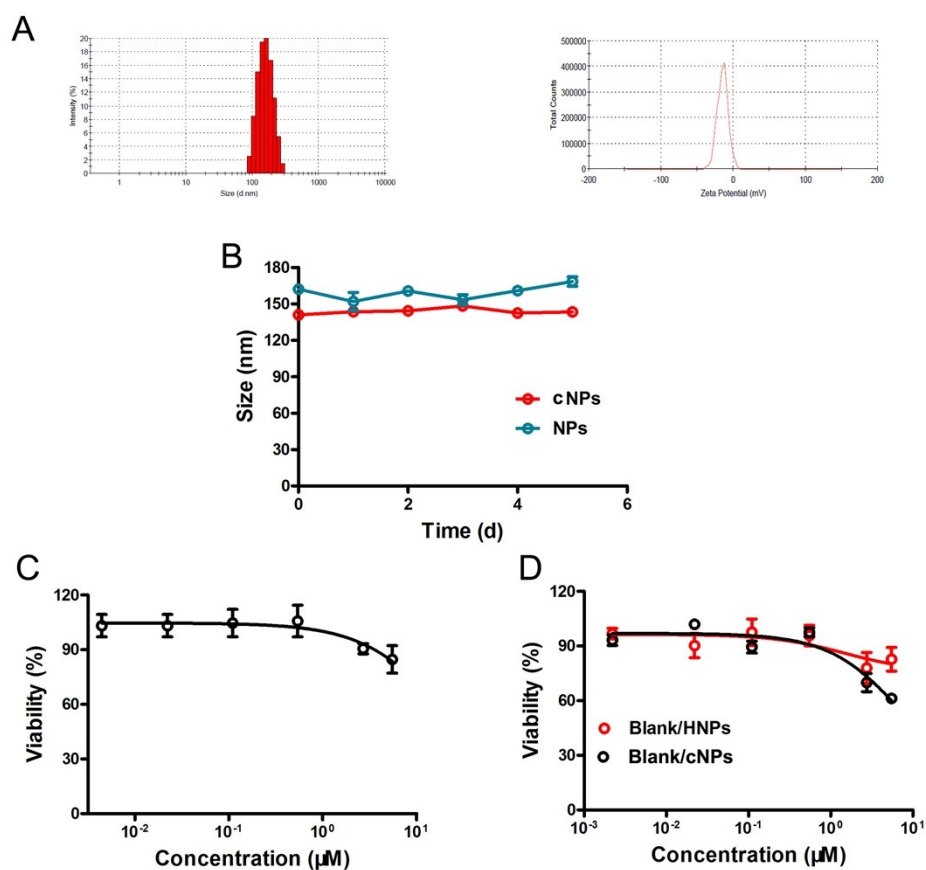


**Figure S4.** (A) Size distributions determined by DLS and surface  $\zeta$  potential of NPs. (B) Size stability of cNPs and NPs. (C) Cytotoxicity study of blank HNPs in Panc02 cells. (D) Cytotoxicity of blank HNPs and CNPs in L929 cells. Data represent mean  $\pm$  SD ( $n = 3$ ).

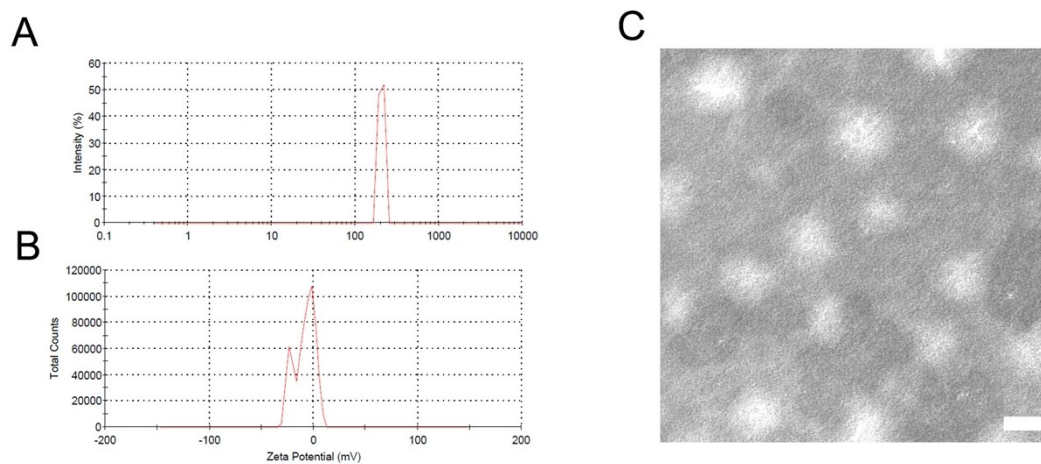


**Figure S5.** (A) Physicochemical characterizations. (A) Size distribution, (B) surface  $\zeta$  potential and (C) morphology of HANase + HNPs determined by DLS and TEM. Scale bars represent 100 nm.

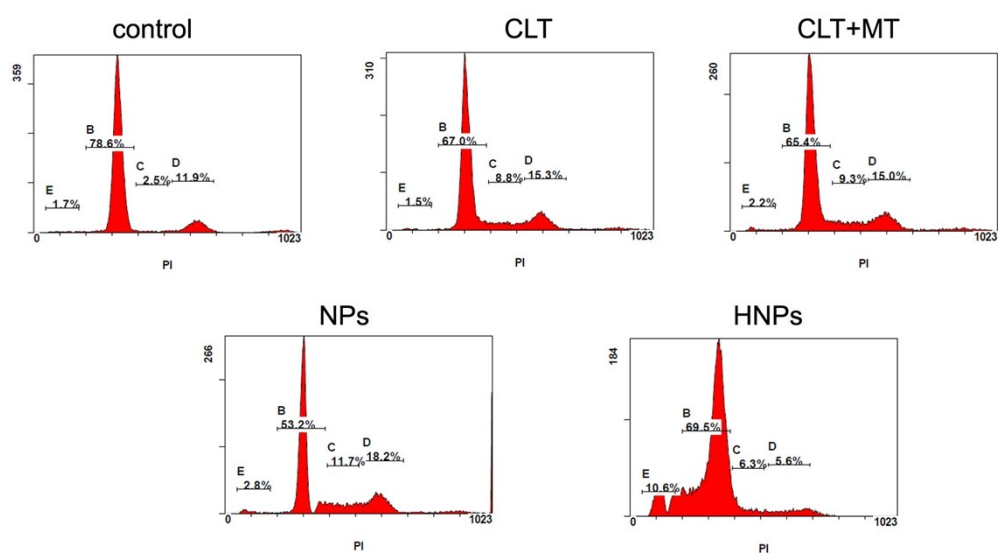


**Figure S6.** Cell cycle analysis of Panc02 cells following different treatments.

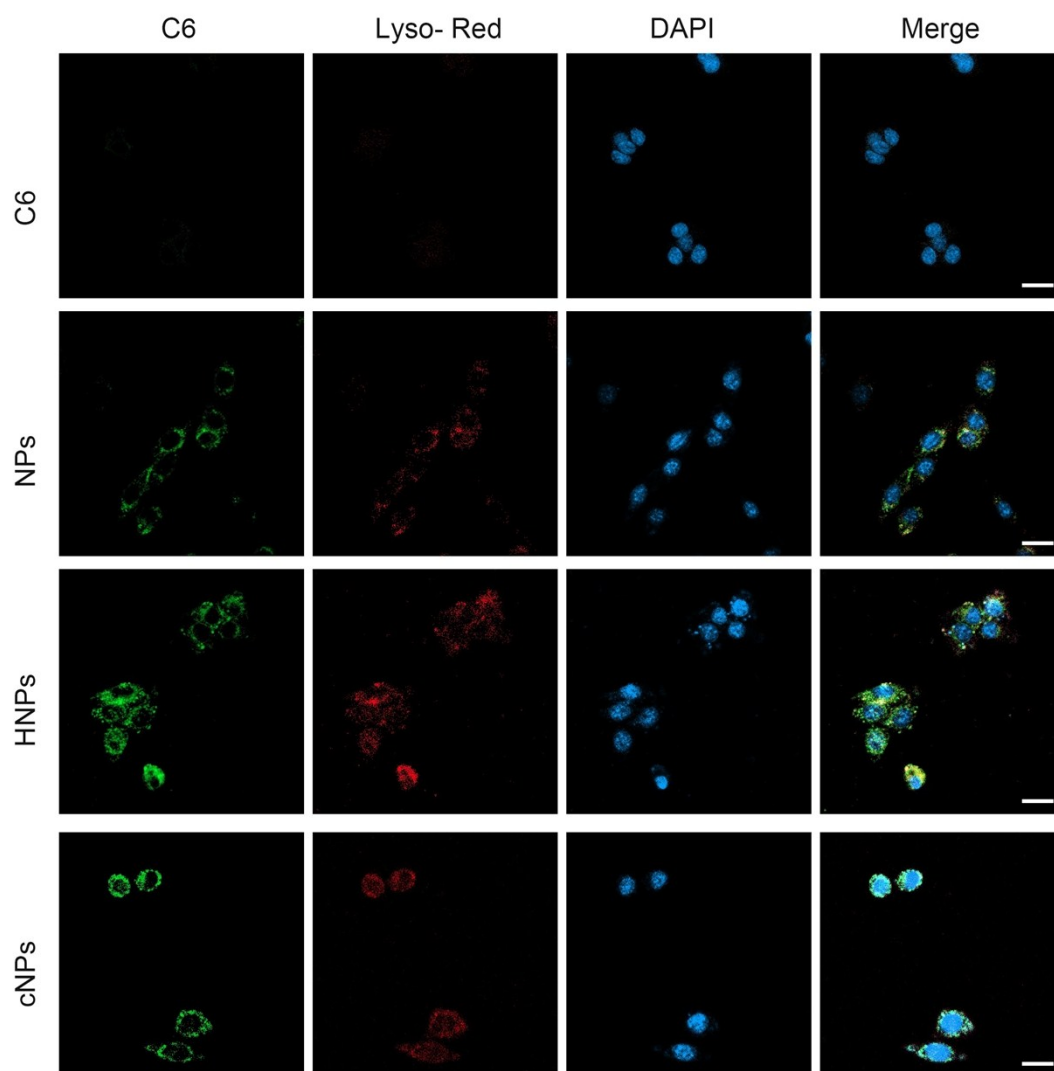


**Figure S7.** *In vitro* cellular uptake. (A) The internalization behaviors of free coumarin-6, NPs, HNPs, and cNPs by

Panc02 cells were quantitatively determined using flow cytometry. (B) Competitive inhibition of internalization of cNPs with chlorpromazine, m- $\beta$ -CD, amiloride, dextran and HA. (C) Representative fluorescence images of free coumarin-6, NPs, HNPs, and cNPs internalized by Panc02 cells, free coumarin-6 as control. Data represent as mean  $\pm$  SD ( $n = 3$ ), \* $P < 0.05$ . Scale bars, 20  $\mu$ m.



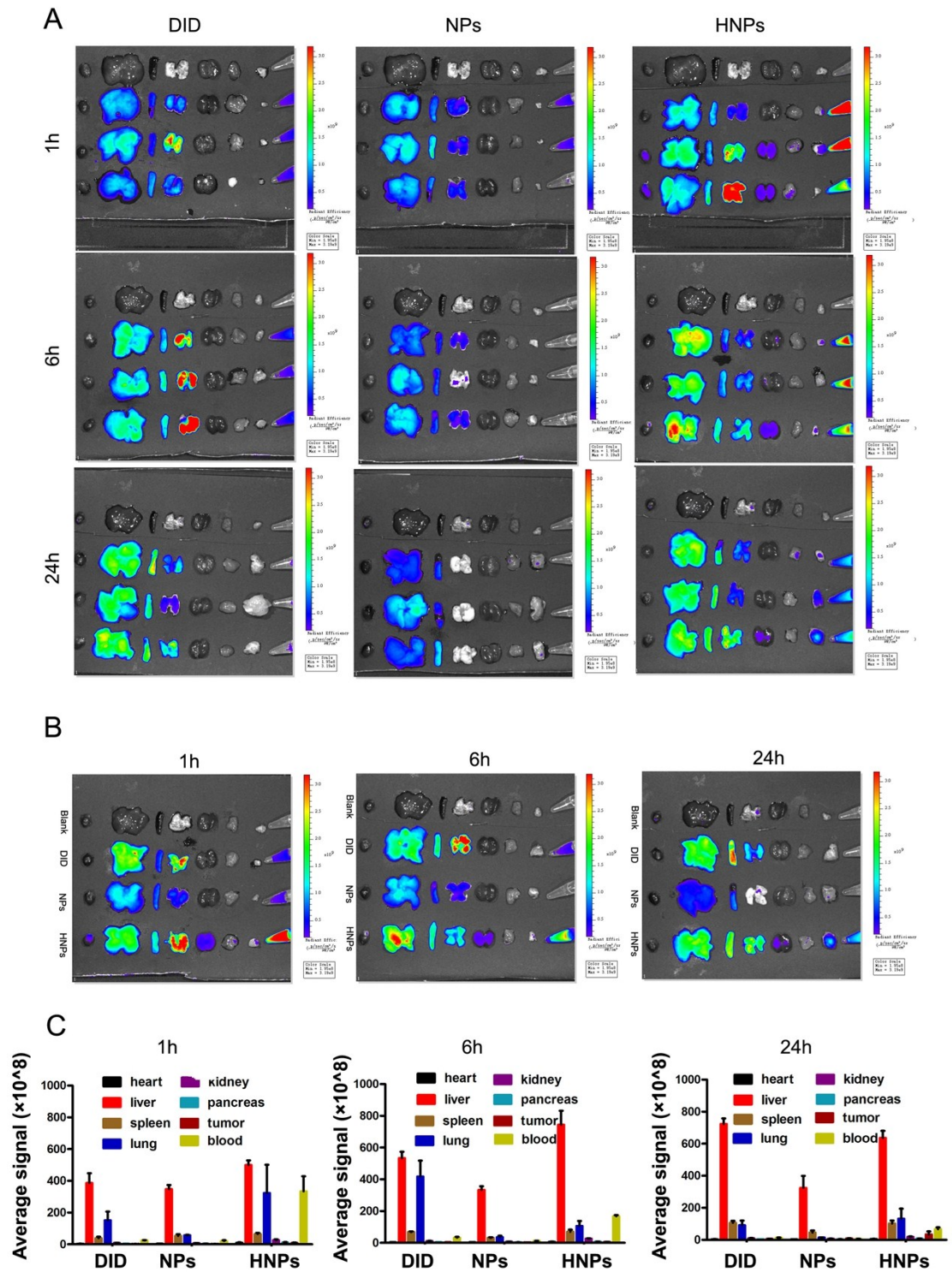


**Figure S8.** *In vivo* distribution. (A) and (B), Representative *in vivo* fluorescence image of major organs from mice sacrificed at the indicated times after *i.v.* injection of DID alone or loaded with NPs or HNPs. (C) The results of semi-quantitative analysis. Data represent mean  $\pm$  SD ( $n = 3$ ).



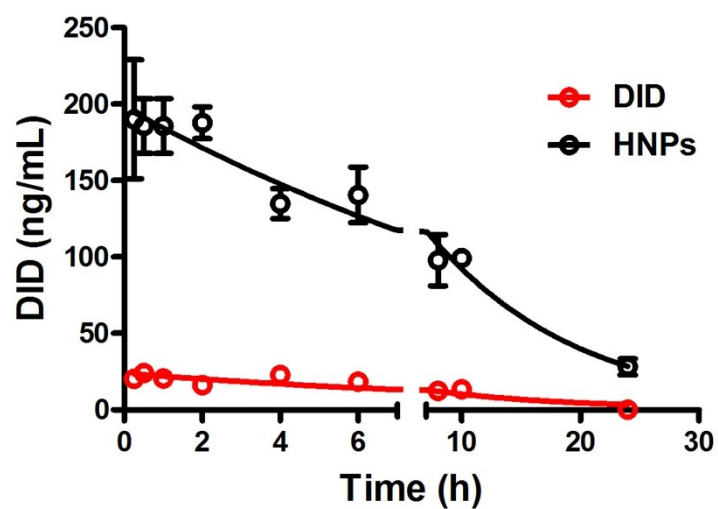


**Figure S9.** Plasma concentration-time profiles of DID following *i.v.* administration of DID solution and HNPs at an equivalent dose of 75  $\mu\text{g/kg}$  of DID. Data represent mean  $\pm$  SD ( $n = 3$ ).

**Table S1.** Summary of pharmacokinetic parameters. Pharmacokinetics parameters were calculated for DID after intravenous injection of DID and HNPs in Panc02 tumor-bearing mice. Data represent mean  $\pm$  SD ( $n = 3$ ).

Parameters	DID	HNPs
$\text{AUC}_{0-t}$ ( $\mu\text{g/L}\cdot\text{h}$ )	312.401	2223.209*
$\text{MRT}_{0-t}$ (h)	7.237	7.73
$t_{1/2z}$ (h)	1.222	6.877*
$C_{\text{max}}$ ( $\mu\text{g/L}$ )	29.92	171.2*
$\text{CL}_z$ ( $\text{L/h/kg}$ )	0.24	0.031

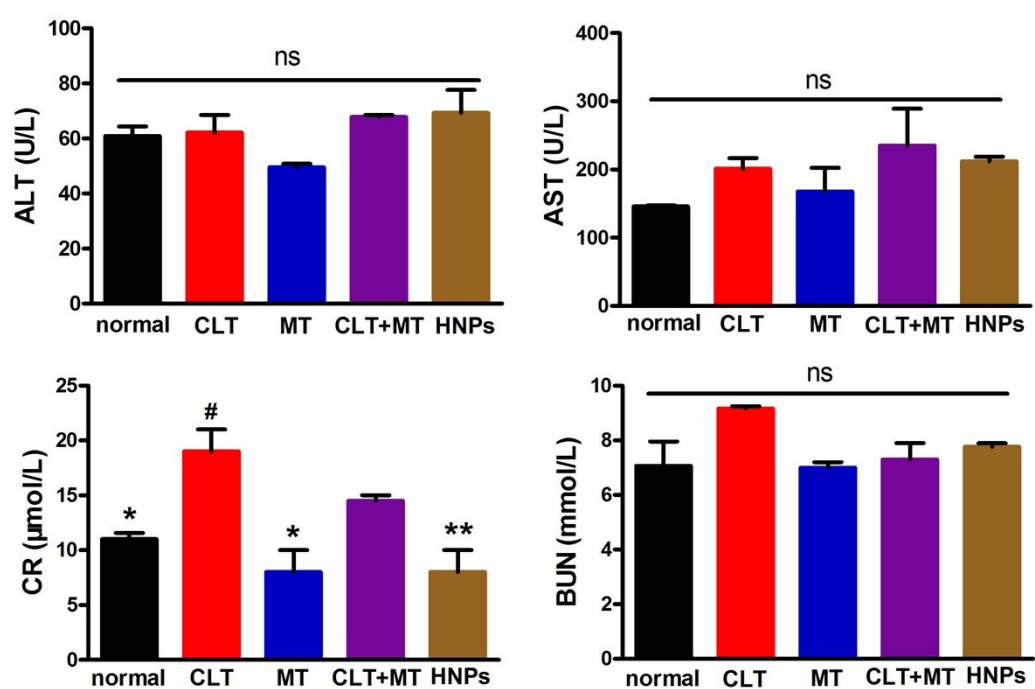


**Figure S10.** Quantitative analysis of biochemical indexes for glutamic pyruvic transaminase (ALT), glutamic-oxalacetic transaminase (AST), creatinine (CR) and urea nitrogen (BUN). Data represent mean  $\pm$  SD (n = 3). \*  $P < 0.05$ , \*\*  $P < 0.01$  vs CLT. #  $P < 0.05$  vs normal group.

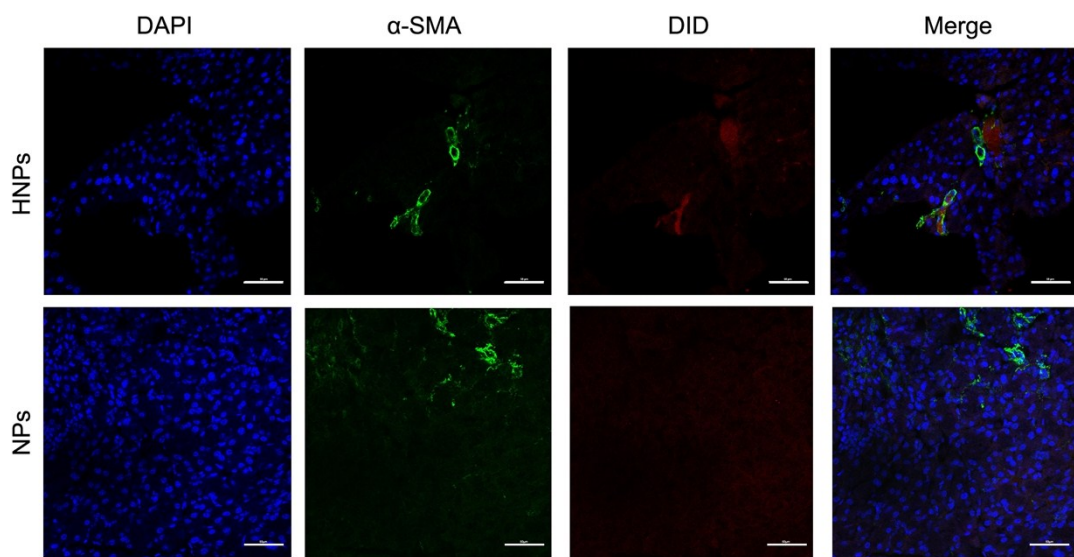


**Figure S11.** Confocal microscopic images for orthotopic pancreatic cancer tissues. Scale bars = 50  $\mu\text{m}$ .

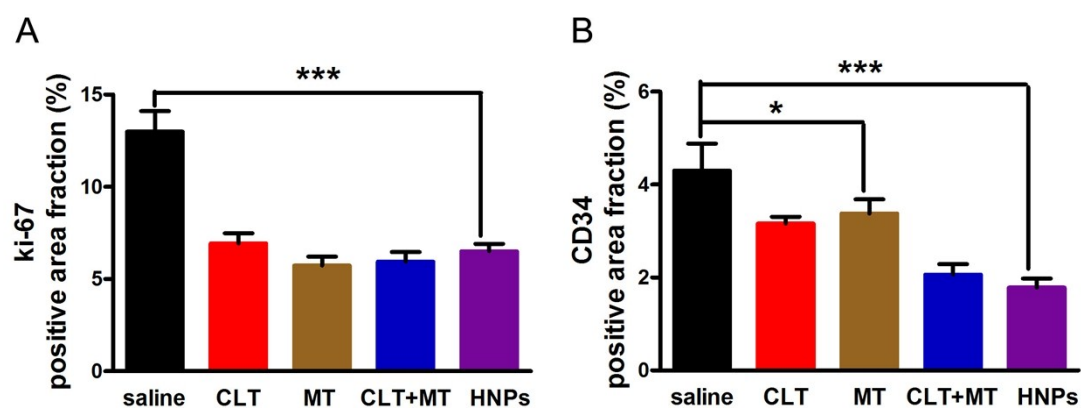


**Figure S12.** Semi-quantitative analysis of Ki-67 and CD34 in Panc02 ectopic tumor model. (A) Ki-67, (B) CD34. \*  $P < 0.05$ ; \*\*\*  $P < 0.005$

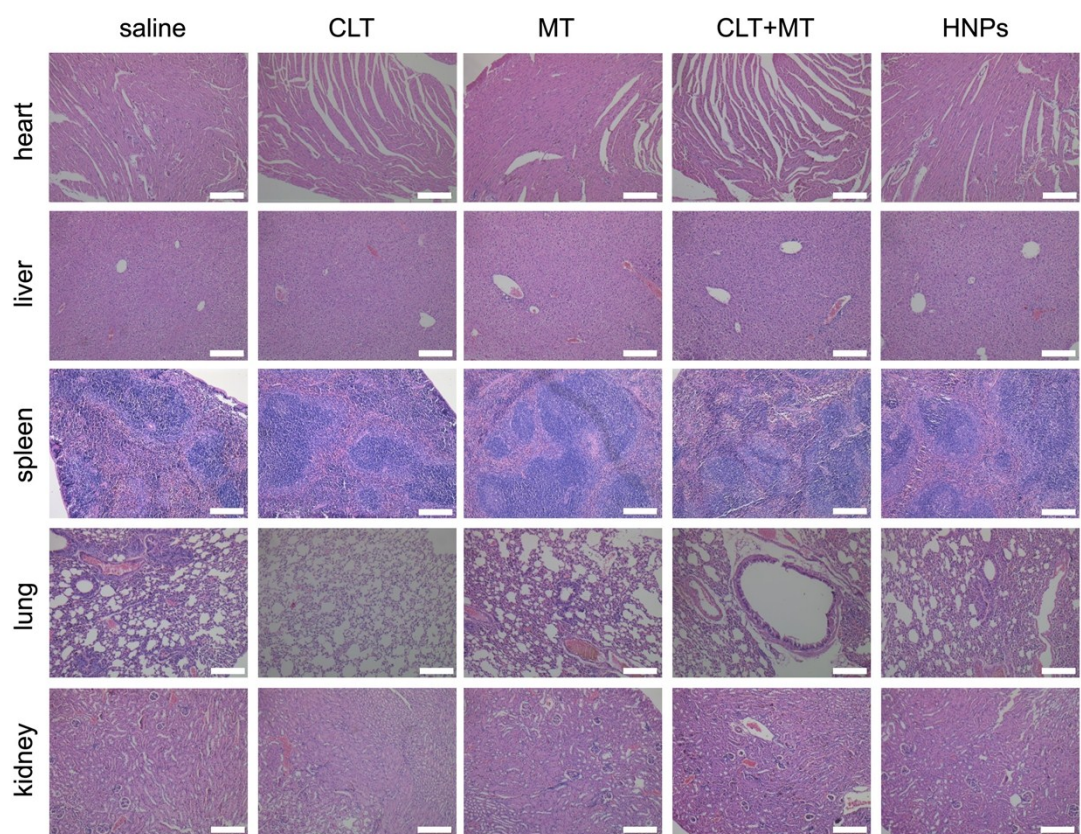


**Figure S13.** Panc02 ectopic tumor model. CLT induces severe cardiotoxicity. Hematoxylin & eosin (H&E) staining assay of heart, liver, spleen, lung and kidney on day 19 after mice sacrificed in Panc02 xenograft model in C57BL/6 mice. Scale bars = 200  $\mu\text{m}$ .



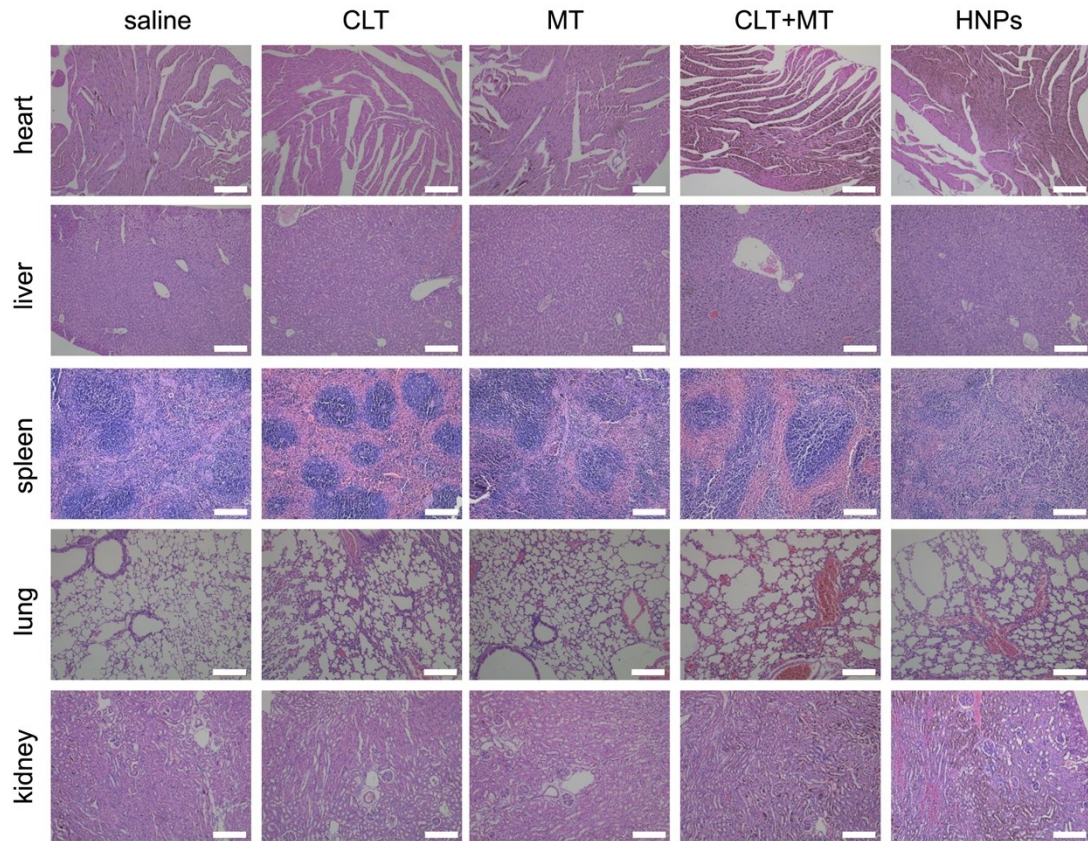


**Figure S14.** Panc02 orthotopic tumor model. CLT induces side effects in various organs. Hematoxylin & eosin (H&E) staining assay of heart, liver, spleen, lung and kidney on day 13 after mice sacrificed in Panc02 orthotopic model in C57BL/6 mice. Scale bars = 200  $\mu$ m.